INL/EXT-14-32547

SUPPLEMENTAL REACTOR PHYSICS CALCULATIONS AND ANALYSIS OF ELF MK 1A FUEL

Michael A. Pope

October 2014

The INL is a U.S. Department of Energy National Laboratory
operated by Battelle Energy Alliance

INL/EXT-14-32547

SUPPLEMENTAL REACTOR PHYSICS CALCULATIONS AND ANALYSIS OF ELF MK 1A FUEL

Michael A. Pope

October 2014

Idaho National Laboratory

Idaho Falls, Idaho 83415

http://www.inl.gov

Prepared for the
U.S. Department of Energy
Office of Nuclear Energy
Under DOE Idaho Operations Office
Contract DE-AC07-05ID14517

Title: Supplemental Reactor Physics Calculations and Analysis of ELF Mk 1A Fuel

ECAR No.: ECAR-2547 Rev. No.: 1 Project No.: 31230 Date: 10/14/2014

1. Quality Level (QL) No.	QL-2	**Professional Engineer's Stamp** See LWP-10010 for requirements.
2. QL Determination No.	QLD-ATR-COMP-000212	
3. Engineering Job (EJ) No.	NA	
4. SSC ID	NA	
5. Building	EROB	
6. Site Area	REC	

7. Objective/Purpose:

These calculations supplement previous the reactor physics work evaluating the Enhanced Low Enriched Uranium (LEU) Fuel (ELF) Mk 1A element. This includes various additional comparisons between the current Highly Enriched Uranium (HEU) and LEU along with further characterization of the performance of the ELF fuel.

8. If revision, please state the reason and list sections and/or pages being affected:

Revision 1, eCR 626395, revised the safety rod worth comparison description in Section 4.6 and updated the associated rod worth values in Table 6.

9. Conclusions/Recommendations:

The excess reactivity to be held down at BOC for ELF Mk 1A fuel is estimated to be approximately $2.75 greater than with HEU for a typical cycle. This is a combined effect of the absence of burnable poison in the ELF fuel and the reduced neck shim worth in LEU fuel compared to HEU. Burnable poison rods were conceptualized for use in the small B positions containing Gd_2O_3 absorber. These were shown to provide $2.37 of negative reactivity at BOC and to burn out in less than half of a cycle. The worth of OSCCs is approximately the same between HEU and ELF Mk 1A (LEU) fuels in the representative loading evaluated. This was evaluated by rotating all banks simultaneously. The safety rod worth is relatively unchanged between HEU and ELF Mk 1A (LEU) fuels in the representative loading evaluated. However, this should be reevaluated with different loadings. Neutron flux, both total and fast (>1 MeV), is either the same or reduced upon changing from HEU to ELF Mk 1A (LEU) fuels in the representative loading evaluated. This is consistent with the well-established trend of lower neutron fluxes for a given power in LEU than HEU. The IPT loop void reactivity is approximately the same or less positive with ELF Mk 1A (LEU) fuel than HEU in the representative loading evaluated.

CONTENTS

Title:	Supplemental Reactor Physics Calculations and Analysis of ELF Mk 1A Fuel						
ECAR No.:	ECAR-2547	Rev. No.:	1	Project No.:	31230	Date:	10/14/2014

1. Project Roles and Responsibilities

Project Role	Name (Typed)	Organization	Pages covered (if applicable)
Performer	Michael A. Pope	C110	All
Checker[a]	Mark D. DeHart	C110	All
Independent Reviewer[b]	David W. Nigg	C100	All
CUI Reviewer[c]	See STIMS Review		All
Manager[d]	Kevin P. Carney	D210	All
Requestor[e]	Sean R. Morrell	D210	All
Nuclear Safety[e]	N/A		All
Document Owner[e]	Sean R. Morrell	D210	All
STIMS Review	See INL/EXT-14-32547		
eCR	626395		

Responsibilities:

a. Confirmation of completeness, mathematical accuracy, and correctness of data and appropriateness of assumptions.

b. Concurrence of method or approach. See definition, LWP-10106.

c. Concurrence with the document's markings in accordance with LWP-11202.

d. Concurrence of procedure compliance. Concurrence with method/approach and conclusion.

e. Concurrence with the document's assumptions and input information. See definition of Acceptance, LWP-10200.

NOTE: *Delete or mark "N/A" for project roles not engaged. Include ALL personnel and their roles listed above in the eCR system. The list of the roles above is not all inclusive. If needed, the list can be extended or reduced.*

Supplemental Reactor Physics Calculations and Analysis of ELF Mk 1A Fuel

Michael A. Pope
Reactor Physics Analysis and Design Department

2. Introduction

A conceptual Low Enriched Uranium (LEU) fuel design has been developed for the Advanced Test Reactor (ATR). This design accomplishes radial power peaking control through adjusted fuel meat thicknesses and no use of burnable poison. Two variations on this Enhanced LEU Fuel (ELF) element have been designed, called ELF Mk 1A and ELF Mk 1B. ELF Mk 1A uses three unique fuel meat thicknesses while ELF Mk 1B uses five unique fuel meat thicknesses to further flatten radial power peaking (at the cost of two additional fuel thicknesses). This document presents physics analysis of ELF Mk 1A only. Because these two designs have nearly identical fuel loadings, none of these results are expected to differ appreciably between the two designs. Table 1 shows fuel meat thicknesses for the Mk 1A fuel. The thickest fuel meat is 16 mils (0.04064 cm) thick and the thinnest fuel meat is 8 mils (0.02032 cm) thick. This variation in thickness compensates for the tendency for peripheral plates to have peaked power as a result of moderation outside the element and shielding of the interior plates. Preliminary physics analyses are presented in Refs. [1] and [2] for ELF Mk 1A and ELF Mk 1B, respectively. Reactor physics calculations were also performed in support of RELAP5 Thermal Hydraulic (TH) analyses. These are presented in Refs. [3] and [4] for ELF Mk 1A and ELF Mk 1B, respectively.

The purpose of these calculations is to supplement the reactor physics work in Ref. [1] with additional comparisons between the current Highly Enriched Uranium (HEU) fuel and the proposed LEU fuel along with further characterization of the performance of the ELF fuel. Reference [1] presented analysis of a representative core loading. This was used to provide a useful comparison of LEU fuel with the current HEU fuel using a reasonable set of simplified conditions. This was a three-batch loading with 18 fresh, 14 once-burned, and 8 twice-burned elements, loaded according to the diagram shown in Figure 1. The same core model was used as a baseline in this work. For a detailed description of this configuration, the reader may refer to Ref. [1]. Descriptions of calculations performed in this work are described by identification of departures from the representative loading from Ref. [1].

Table 1. Fuel meat thicknesses for ELF Mk 1A fuel elements.

Parameter		ELF Mk 1A	
		(cm)	(mils)
Meat Thickness by Plate #	1	0.02032	8
	2	0.03302	13
	3	0.03302	13
	4	0.04064	16
	5	0.04064	16
	6	0.04064	16
	7	0.04064	16
	8	0.04064	16
	9	0.04064	16
	10	0.04064	16
	11	0.04064	16
	12	0.04064	16
	13	0.04064	16
	14	0.04064	16
	15	0.04064	16
	16	0.03302	13
	17	0.02032	8
	18	0.02032	8
	19	0.02032	8
Number of unique thicknesses		3	

3. Modeling Approach

The calculations reported herein were performed using Serpent Version 2.1.15 (July 31, 2013). [5] This is a pre-release *beta* version of this software package; however, all source code and the executable are controlled at INL. The software has not yet been formally qualified for safety analysis, and calculations reported here may not be used in Level 1 quality-controlled analysis. Verification and validation of Serpent are in progress under the LEU Conversion Project as well as under the separate, but directly related, ATR Physics Modeling Update Project for use in such work, and validation analyses completed to date provide confidence in Serpent calculations at a level that is consistent with QA-2 level work per applicable INL Engineering Procedures.

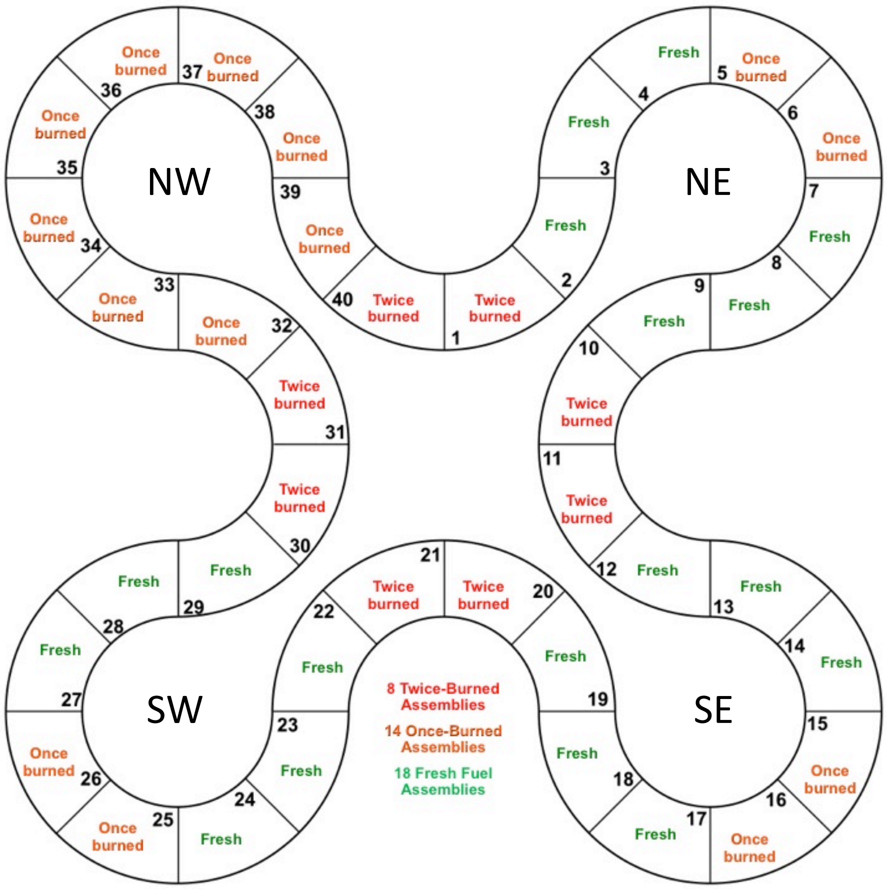

Figure 1. Representative core loading diagram.

All calculations were performed using ENDF/B-VII.0 cross sections as distributed with the Serpent 1.1.7 package via the Radiation Safety Information Computational Center (RSICC) [5]. The only exception to this was the beryllium metal thermal scattering date, which came from ENDF-V. The base model used for these calculations is based on the 94-CIC benchmark described in [6]. Analysis and definition of the original ELF fuel design is provided in [7]. The model used in this work had two neck-shims withdrawn (22 inserted) as was originally used in the 94-CIC benchmark [6] unless otherwise stated. Outer Shim Control Cylinders (OSCCs) were maintained at an 80° rotation unless otherwise stated.

4. Results

4.1. Alternative Core Loadings

In the physics analysis in Ref. [1], the representative loading in Figure 1 was used to compare the burnup capability of ELF Mk 1A (LEU) fuel compared to HEU. This was aimed at demonstrating that the same or greater cycle length could be achieved with the new fuel. It was concluded that for the same representative loading, the ELF Mk 1A (LEU) fuel had more reactivity than the HEU fuel. The difference was approximately $3 additional at beginning of cycle (BOC) and $1 at end-of-cycle (EOC). It was suggested in Ref. [1] that alternative loadings could be used with ELF fuel wherein fewer fresh elements are used while achieving the same cycle length as with HEU. Here, this hypothesis was tested using Serpent depletion calculations. Two alternative loading configurations are presented here giving the same EOC reactivity as the HEU core. One, here referred to as "alternative 2" replaces fresh elements in locations 19 and 22 with twice-burned elements. The other, referred to as "alternative 3" replaces fresh elements in locations 12, 19, 22, and 29 with once-burned elements. Figure 2 shows k_{eff} v. burnup in days for the representative depletion with HEU with ELF Mk 1A (LEU) fuels. The two alternative loadings are also shown in the plot.

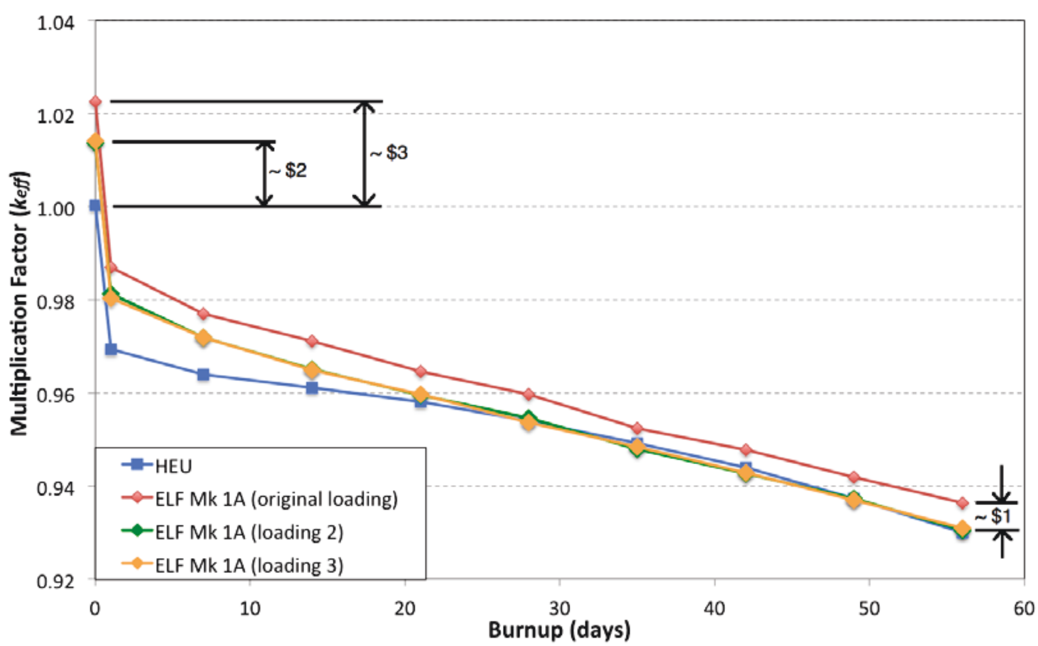

Figure 2. Multiplication factor v. burnup for HEU and ELF Mk 1A with three different loadings.

Both of these alternative ELF Mk 1A loadings give approximately $2 higher reactivity than HEU at BOC and the same reactivity as HEU at EOC. This suggests that these alternative loadings allow ELF Mk 1A fuel to achieve the same cycle length as HEU fuel with 2 to 4 fewer fresh elements loaded per cycle. It should be noted, however, that neck shims are not withdrawn during this simulated depletion. This means that differences in neck shim worth between HEU and LEU are not accounted for here. Any reduction in worth of neck shims or OSCCs from changing to LEU fuel must be compensated for by additional hold-down at BOC. It will be shown that the neck shim worth is diminished somewhat with the change to LEU fuel, and so additional consideration must be made for compensating for this. This is discussed in Section 4.4.

4.2. Burnable Poison Rods in Small B Positions

Because ELF fuel has higher initial reactivity than HEU, and it does not have burnable poison in the fuel element, additional reactivity hold-down must be achieved through either manipulation of OSCCs or by addition of burnable poison external to the fuel elements. Here, a burnable poison rod is conceptualized for insertion into small B positions. The selection of Gd_2O_3 for the burnable absorber was based on a balancing of high worth and ability to burn out in less than one cycle. A schematic of the pin is shown in Fig. 3 and the dimensions are given in Table 2. This current concept uses a 0.005 cm thick shell of Gd_2O_3 with aluminum cladding inside and out. A central coolant channel is specified for this analysis. The aluminum would need to lend some strength because this burnable absorber would also need to serve the function of the B Hole Retainer (INL drawing no. 403205). The function of the B Hole Retainer is to hold a section of aging beryllium in place in the event that it cracks during a cycle. It is used in sections of reflector at high neutron fluence toward the end of the beryllium lifetime. Further design and analysis should be performed in order to produce a viable design serving both of these functions. This is only a feasibility study meant to evaluate the reactivity worth that can be achieved while assuming that the structural function can be served.

Table 3 shows the reactivity worth of a B-hole absorber pin in each of the small B locations, and in all of them simultaneously. These pins have between -$0.16 and -$0.41 of reactivity worth, depending on location. Because the power is concentrated in the southern lobes, the B positions adjacent to the SE and SW lobes have higher worth than those adjacent to the NE and NW lobes. The worth absorber pins in all 8 small B-holes simultaneously is -$2.37.

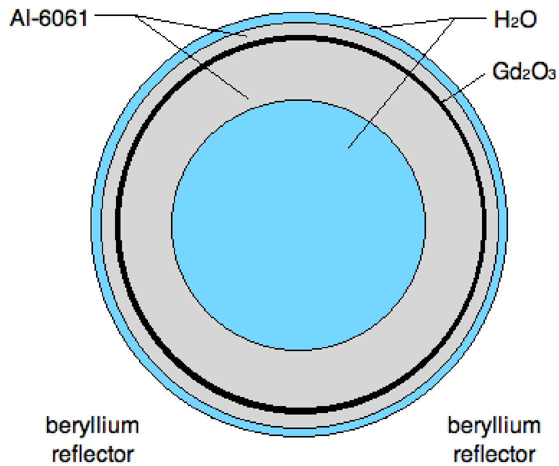

Figure 3. Diagram of B-hole poison pin.

Table 2. Parameters of B-hole absorber poison pin.

Component Surface	**Radius (cm)**
Small B Position	1.11
Pin Outer	1.060
Gd_2O_3 Outer	0.850
Gd_2O_3 Inner	0.845
Inner Coolant Channel	0.500

Table 3. Results from Analysis of Gd_2O_3 absorbers in Small B Positions.

Gd_2O_3 Absorber Locations	**Lobe Adjacent**	k_{eff} *	**Worth ($)** **
None	—	1.02175	—
B1	NE	1.02033	-0.20
B2	NE	1.01987	-0.26
B3	SE	1.01920	-0.35
B4	SE	1.01879	-0.41
B5	SW	1.01886	-0.40
B6	SW	1.01964	-0.29
B7	NW	1.02029	-0.20
B8	NW	1.02060	-0.16
All small B positions	All	1.00494	-2.37

* ± 0.00009

** ± $0.02

4.3. Depletion with External Burnable Poison Pins

The burnable poison pin design evaluated above was used in depletion analyses of the cores with modified loadings presented in Section 4.1. The purpose of this is to demonstrate that the burnable poisons proposed in Section 4.2 burn out in less than one cycle. This analysis is performed with all but two neck shims inserted and the OSCCs rotated to 80º, as in the representative depletion in [1] and in Section 4.1 of this report. Figure 4 shows k_{eff} v. burnup for the HEU representative depletion along with the two LEU alternative loadings with poisons in 6 of the 8 small B locations. This shows that by 20 days, the poisons are depleted and the reactivity at end of cycle is similar to that of HEU. Again, it should be noted that the difference in reactivity worth of neck shims and OSCCs are treated separately in Sections 4.4 and 4.5. These analyses must be taken into consideration for a more complete understanding of the additional reactivity hold-down requirements of converting to ELF Mk 1A fuel.

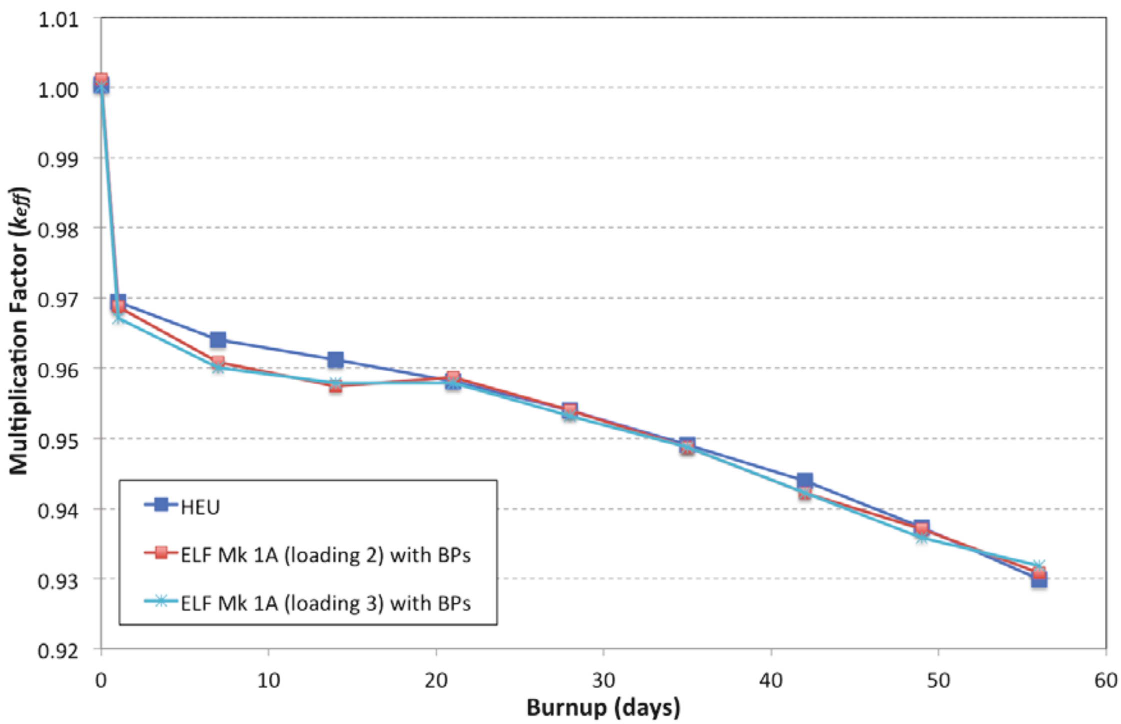

Figure 4. Multiplication factor v. burnup for HEU and ELF Mk 1A with two alternative loadings and burnable absorber pins in positions B2-B7.

4.4. Neck Shim Worth Comparison

Comparisons were performed between neck shim worth in HEU and ELF Mk 1A (LEU) fueled cores. The representative loadings were used all neck shims were inserted in the nominal case. Neck shims were then withdrawn individually and the reactivity increase was recorded as the neck shim worth. For this analysis, regulating rods were treated exactly the same as ordinary neck shims. Each time a neck shim was withdrawn, the previous one was re-inserted. Therefore, only one was modeled as withdrawn at any given time. Then all neck shims were withdrawn simultaneously giving their collective worth. Table 4 shows neck shim worths in the HEU and ELF Mk 1A (LEU) loaded cores.

The worth of nearly all neck shims either remained the same (within statistical uncertainty of the Serpent calculations) or diminished upon changing from HEU to ELF Mk 1A (LEU) fuel. At BOC in ATR, nearly all neck shims are inserted (all but two regulating rods) and at EOC, nearly all neck shims are withdrawn (again all but two regulating rods). The worth of all neck shims inserted was found to be about 521 pcm (~ $0.75) less in the LEU fuel than with HEU.

The representative depletion from [1] and the alternative loadings in Sections 4.1 and 4.3 of this report have all but two neck shims inserted. This means that at the end of cycle, approximately $0.75 of reactivity must be credited to the HEU fuel in this comparison. Thus, in Figure 2, when the representative loading of ELF Mk 1A fuel has approximately $1 additional reactivity at EOC compared to HEU, it is actually nearly the same reactivity for the purposes of this analysis. Therefore, a loading intermediate to the original representative loading and the alternatives (although closer to the original representative loading) may be a viable option. Also, in determining the additional reactivity holddown at BOC for ELF Mk 1A fuel, the original representative loading shown in Figure 2 is more close to the actual value. Considering the neck shim value, then, the additional holddown required for ELF Mk 1A fuel is estimated to be approximately $2.75. In Section 4.2, it was shown that if all eight small B positions could be occupied by the proposed burnable poison, this would give -$2.37 of holddown. If OSCCs can be rotated inward (lower numerical rotation) at BOC than normally done, some of this additional holddown could be accommodated, reducing the burden on external burnable poisons and occupying fewer test positions.

Table 4. Neck shim worth in HEU and ELF Mk 1A cores.

Neck Shim(s) Withdrawn	**HEU** (β_{eff} = 0.00701)			**LEU** (β_{eff} = 0.00692)			**Δ Worth*** **(LEU – HEU)** in pcm (± 17 pcm)
	k_{eff} (± 8E-5)	Worth (pcm)	Worth ($)	k_{eff} (± 6E-5)	Worth (pcm)	Worth ($)	
None	0.99654	NA	NA	1.01790	NA	NA	NA
SW1	0.99842	189	0.27	1.01930	135	0.19	-54
SW2	0.99830	176	0.25	1.01930	135	0.19	-41
SW3	0.99822	169	0.24	1.01965	169	0.24	0
SW4	0.99819	166	0.24	1.01944	148	0.21	-17
SW5	0.99856	203	0.29	1.01964	168	0.24	-35
SW6	0.99869	215	0.31	1.02002	204	0.29	-11
SE1	0.99831	178	0.25	1.01954	158	0.23	-20
SE2	0.99816	162	0.23	1.01947	151	0.22	-11
SE3	0.99830	176	0.25	1.01943	147	0.21	-29
SE4	0.99819	166	0.24	1.01957	161	0.23	-5
SE5	0.99837	183	0.26	1.01966	170	0.24	-14
SE6	0.99873	220	0.31	1.02008	210	0.30	-10
NW1	0.99794	141	0.20	1.01914	120	0.17	-21
NW2	0.99802	149	0.21	1.01899	105	0.15	-43
NW3	0.99768	115	0.16	1.01892	98	0.14	-16
NW4	0.99802	149	0.21	1.01883	90	0.13	-59
NW5	0.99768	114	0.16	1.01890	96	0.14	-18
NW6	0.99791	138	0.20	1.01899	105	0.15	-32
NE1	0.99803	150	0.21	1.01918	123	0.18	-26
NE2	0.99776	123	0.17	1.01900	106	0.15	-17
NE3	0.99774	121	0.17	1.01916	121	0.18	1
NE4	0.99777	123	0.18	1.01910	116	0.17	-7
NE5	0.99776	122	0.17	1.01938	143	0.21	21
NE6	0.99791	137	0.20	1.01963	167	0.24	30
Average	NA	158	0.22	NA	139	0.20	-18
All Neck Shims Withdrawn	1.04674	4812	6.86	1.06439	4291	6.20	-521

* Negative values indicate that neck shim has lower worth with LEU than with HEU fuel.

4.5. OSCC Worth Comparison

Comparisons were also performed between OSCC worth in HEU and ELF Mk 1A fueled cores. The representative loadings were used and all OSCC banks were rotated simultaneously from 0º to 180º in 10º increments. Table 5 shows results of this study with a comparison of worths of OSCC rotation using 180º as a baseline. This shows that the difference in OSCC worth between HEU and ELF Mk 1A (LEU) is less than 100 pcm for most rotations. This is not anticipated to present a major challenge to operational practices.

Table 5. Worth of simultaneous rotation of OSCCs in HEU and ELF Mk 1A cores.

OSCC Rotation (degrees)	**HEU** (β_{eff} = 0.00701)			**LEU** (β_{eff} = 0.00692)			**Δ (LEU – HEU)** in pcm (± 15 pcm)
	k_{eff} (± 8E-5)	Worth (pcm)	Worth ($)	k_{eff} (± 6E-5)	Worth (pcm)	Worth ($)	
0	0.94355	-10451	-14.90	0.96353	-10336	-14.93	115
10	0.94535	-10250	-14.61	0.96544	-10132	-14.64	118
20	0.94876	-9870	-14.07	0.96865	-9788	-14.14	82
30	0.95389	-9303	-13.26	0.97376	-9246	-13.36	57
40	0.96060	-8570	-12.22	0.98078	-8512	-12.30	59
50	0.96952	-7613	-10.86	0.98940	-7623	-11.01	-10
60	0.97961	-6550	-9.34	0.99968	-6583	-9.51	-33
70	0.99024	-5454	-7.78	1.01051	-5512	-7.96	-57
80	1.00091	-4378	-6.24	1.02141	-4456	-6.44	-78
90	1.01100	-3381	-4.82	1.03192	-3458	-5.00	-77
100	1.02019	-2490	-3.55	1.04145	-2572	-3.72	-82
110	1.02821	-1725	-2.46	1.04978	-1810	-2.61	-84
120	1.03471	-1114	-1.59	1.05679	-1178	-1.70	-63
130	1.03982	-639	-0.91	1.06233	-684	-0.99	-45
140	1.04350	-300	-0.43	1.06646	-320	-0.46	-20
150	1.04601	-70	-0.10	1.06930	-71	-0.10	0
160	1.04724	42	0.06	1.07069	51	0.07	9
170	1.04744	60	0.09	1.07082	62	0.09	2
180	1.04678	0	0.00	1.07011	0	0.00	0

4.6. Safety Rod Worth Comparison

Comparisons were also performed evaluating the worths of safety rods between HEU and ELF Mk 1A (LEU) fueled cores. Again using the representative core as a baseline, safety rods were inserted both individually and simultaneously. When withdrawn, safety rods are actually 3 inches inserted into the active fuel region from the top of the core. At full insertion, the rod has been moved down into the active core by 36 inches (i.e., the bottom of the safety rod is then located 39 inches below the top of the active fuel and is 9 inches above the bottom of the fuel).. Table 6 shows worths of individual safety rods and the worth of all six inserted simultaneously. This showed that there was some variation in the worths of individual safety rods between the two cores. In ATR safety analysis, credit is taken for the sum of the individual worths of the five lowest-worth safety rods.

[8] The average value of this is given as $13.3, while the worth of all six rods is reported to be $17. [8] The sum of all six rod worths is given in Table 6 for both HEU and LEU, as is the sum of the worths of the five least valuable rods (omitting the East rod). The sum of the worths of the five least valuable rods was calculated to be $14.4 in the HEU core and $13.8 in the LEU core. This represents a 4% reduction in safety rod worth.

Table 6. Safety rod worth comparison between HEU and ELF Mk 1A (LEU) fuel in representative loading.

Safety Rod Inserted	**HEU** (β_{eff} = 0.00701)			**LEU** (β_{eff} = 0.00692)			**Δ (LEU – HEU)*** in $
	k_{eff} (± 8E-5)	Worth (pcm)	Worth ($)	k_{eff} (± 6E-5)	Worth (pcm)	Worth ($)	
None	1.00104	NA	NA	1.02175	NA	NA	NA
N	0.98602	1521	2.17	1.00814	1321	1.91	-0.26
W	0.98090	2051	2.93	1.00359	1771	2.56	-0.37
E	0.97240	2942	4.19	0.99218	2917	4.21	0.02
S	0.97980	2166	3.09	0.99926	2203	3.18	0.09
SW	0.98010	2134	3.04	1.00126	2003	2.89	-0.15
SE	0.97923	2225	3.17	0.99850	2279	3.29	0.12
All Inserted	0.86423	15814	22.55	0.88446	15192	21.95	-0.60
Sum of all 6	—	1304	18.6	—	1249	18.0	-0.54
Sum of 5**	—	1010	14.4	—	958	13.8	-0.56

* Positive values indicate that safety rod has lower worth with LEU than with HEU fuel.
** Highest worth rod omitted as per SAR.

4.7. Neutron Flux in Beryllium Reflector

Calculations were performed to evaluate the impact of changing to ELF Mk 1A (LEU) fuel on flux levels in the beryllium reflector. This has implications for neutron damage and, ultimately, the frequency with which the reflector must be replaced. Thin portions of beryllium reflector called “ligaments” separate fuel from OSCCs in various locations. Because these portions of reflector are structurally weak and due to the high neutron fluence that they experience, ligaments are important in the determination of when the beryllium reflector is anticipated to fail. The reflector is also fabricated into sharp points near each of the small B positions. This is also a region of interest with regard to neutron damage. Sample locations were selected from these regions for this analysis.

Figure 5 shows the locations of ligaments “A” and “E” in the southeast lobe. Serpent was used to tally the neutron flux in these positions for the representative core loading at

120 MW. This was also done for the B3 and B4 positions, also shown in Figure 5. The analogous positions in the northwest lobe were also tallied. Neutron flux was divided into that above 1 MeV, below 1 MeV, and total. The tally regions were 20 cm tall and located at the axial center of the active fuel.

Table 7 shows neutron flux in these positions in the beryllium reflector for ELF Mk 1A (LEU) fuel. For both lobes, the raw numbers are presented followed by the values scaled to a 60 MW lobe in order to provide a fair comparison. Fluxes are broken into three columns: below 1 MeV, above 1 MeV, and total flux. Table 8 shows the same data for the HEU-fueled core. Table 9 shows the difference between HEU and LEU in percent for each of the locations with the associated lobe power scaled to 60 MW. This shows that the fast flux has either stayed the same (within statistical uncertainty) or decreased in all cases when HEU is replaced by the ELF Mk 1A (LEU) fuel. Thermal and total fluxes have decreased in all of the tallied locations when HEU is replaced by the ELF Mk 1A (LEU) fuel. This is consistent with the general trend of lower flux levels typical of a conversion from HEU to LEU fuel.

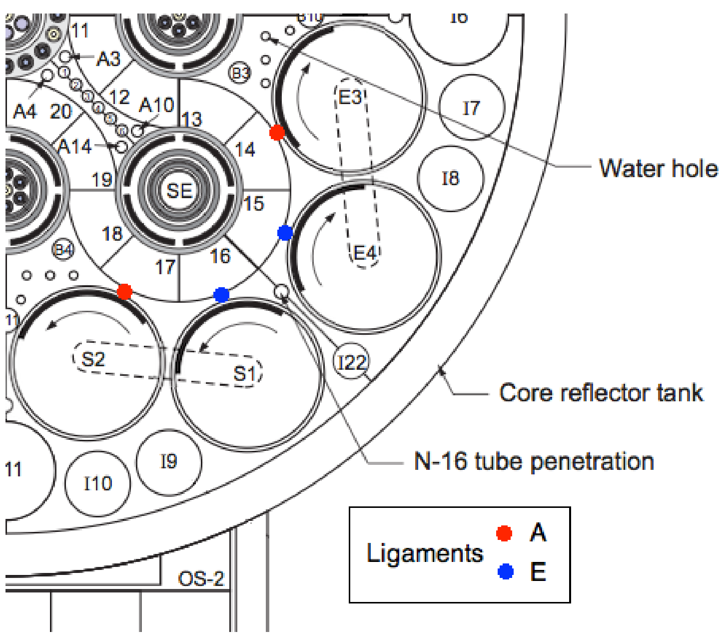

Figure 5. SE Lobe with high flux ligaments labeled.

Table 7. Neutron flux in various positions in beryllium reflector for ELF Mk 1A fuel.

Lobe (power)	Location Type	Adjacent Element	Neutron Flux ($n\cdot cm^{-2}\cdot s^{-1}$) At calculated lobe power			Neutron Flux ($n\cdot cm^{-2}\cdot s^{-1}$) Scaled to 60 MW Lobe Power		
			< 1 MeV	> 1 MeV	Total	< 1 MeV	> 1 MeV	Total
SE (29.5 MW)	A ligament	17	9.33E+14	1.77E+14	1.11E+15	1.89E+15	3.58E+14	2.25E+15
	A ligament	14	9.02E+14	1.74E+14	1.08E+15	1.83E+15	3.53E+14	2.18E+15
	E ligament	16	7.83E+14	1.52E+14	9.35E+14	1.59E+15	3.08E+14	1.90E+15
	E ligament	15	7.70E+14	1.51E+14	9.21E+14	1.56E+15	3.06E+14	1.87E+15
	B3 position	13	9.65E+14	1.30E+14	1.10E+15	1.96E+15	2.64E+14	2.22E+15
	B4 position	18	1.03E+15	1.40E+14	1.17E+15	2.08E+15	2.83E+14	2.36E+15
NW (17.3 MW)	A ligament	34	5.43E+14	9.79E+13	6.40E+14	1.88E+15	3.39E+14	2.22E+15
	A ligament	37	5.22E+14	9.66E+13	6.18E+14	1.81E+15	3.35E+14	2.14E+15
	E ligament	35	4.26E+14	8.02E+13	5.06E+14	1.48E+15	2.78E+14	1.76E+15
	E ligament	36	4.26E+14	8.28E+13	5.09E+14	1.48E+15	2.87E+14	1.76E+15
	B7 position	33	6.99E+14	9.09E+13	7.90E+14	2.42E+15	3.15E+14	2.74E+15
	B8 position	38	6.39E+14	8.32E+13	7.22E+14	2.21E+15	2.88E+14	2.50E+15

Table 8. Neutron flux in various positions in beryllium reflector for HEU fuel.

Lobe (power)	Location Type	Adjacent Element	Neutron Flux ($n\cdot cm^{-2}\cdot s^{-1}$) At calculated lobe power			Neutron Flux ($n\cdot cm^{-2}\cdot s^{-1}$) Scaled to 60 MW Lobe Power		
			< 1 MeV	> 1 MeV	Total	< 1 MeV	> 1 MeV	Total
SE (28.4 MW)	A ligament	17	9.58E+14	1.76E+14	1.13E+15	2.02E+15	3.72E+14	2.39E+15
	A ligament	14	9.26E+14	1.73E+14	1.10E+15	1.95E+15	3.63E+14	2.31E+15
	E ligament	16	8.41E+14	1.57E+14	9.98E+14	1.77E+15	3.32E+14	2.10E+15
	E ligament	15	8.32E+14	1.57E+14	9.89E+14	1.75E+15	3.30E+14	2.08E+15
	B3 position	13	9.74E+14	1.32E+14	1.11E+15	2.05E+15	2.77E+14	2.33E+15
	B4 position	18	1.04E+15	1.41E+14	1.18E+15	2.19E+15	2.97E+14	2.49E+15
NW (19.6 MW)	A ligament	34	6.73E+14	1.23E+14	7.96E+14	2.05E+15	3.75E+14	2.42E+15
	A ligament	37	6.45E+14	1.19E+14	7.64E+14	1.97E+15	3.62E+14	2.33E+15
	E ligament	35	5.51E+14	1.05E+14	6.56E+14	1.68E+15	3.19E+14	2.00E+15
	E ligament	36	5.43E+14	1.00E+14	6.44E+14	1.66E+15	3.05E+14	1.96E+15
	B7 position	33	8.14E+14	1.04E+14	9.18E+14	2.48E+15	3.17E+14	2.80E+15
	B8 position	38	7.42E+14	9.59E+13	8.38E+14	2.26E+15	2.92E+14	2.55E+15

Table 9. Difference in neutron flux at various positions in beryllium reflector between HEU and LEU.

Lobe	Location Type	Adjacent Element Number	Neutron Flux Change (%) Scaled to 60 MW Lobe Power		
			< 1 MeV	> 1 MeV	Total
SE	A ligament	17	-6.3 ± 0.7	-3.6 ± 1.8	-5.8 ± 0.7
	A ligament	14	-6.3 ± 0.7	-2.7 ± 1.8	-5.7 ± 0.7
	E ligament	16	-10.3 ± 0.7	-7.1 ± 2.0	-9.8 ± 0.7
	E ligament	15	-10.9 ± 0.7	-7.1 ± 2.0	-10.3 ± 0.7
	B3 position	13	-4.6 ± 0.5	-4.8 ± 0.9	-4.6 ± 0.5
	B4 position	18	-5.2 ± 0.5	-4.6 ± 0.9	-5.1 ± 0.5
NW	A ligament	34	-8.2 ± 0.8	-9.5 ± 2.4	-8.4 ± 0.8
	A ligament	37	-7.9 ± 0.8	-7.4 ± 2.4	-7.9 ± 0.8
	E ligament	35	-12.0 ± 0.9	-12.7 ± 2.7	-12.1 ± 0.9
	E ligament	36	-10.8 ± 0.9	-5.8 ± 2.7	-10.0 ± 0.9
	B7 position	33	-2.2 ± 0.5	-0.4 ± 1.1	-2.0 ± 0.5
	B8 position	38	-2.0 ± 0.5	-1.2 ± 1.1	-1.9 ± 0.5

4.8. Neutron Flux in IPT Pressure Tubes

A similar calculation to that described in Section 4.7 was performed, but to determine the change in neutron flux in In-Pile-Tubes (IPTs) resulting from changing from HEU to ELF Mk 1A (LEU) fuel. Tallies were performed using the representative HEU and ELF Mk 1A (LEU) loadings. Tallies were located at the axial center of the core and 20 cm in height. Fluxes were again divided into >1 MeV, < 1 MeV, and total. Table 10 shows Neutron flux in IPT pressure tubes for ELF Mk 1A (LEU) fuel. For the SW, SE, and NW IPTs, the raw numbers are given along with those resulting from normalizing their corresponding lobe power to 60 MW. The N and W flux traps do not have a true eight-element lobe surrounding them. In these cases, the six adjacent element powers were summed and then scaled to 45 MW for comparison. Table 11 shows the same values for HEU fuel and Table 12 shows the percent differences between HEU and ELF Mk 1A. The N and W IPTs do not have a normalized value because they are not associated with one particular lobe. The percent change in raw value is given in Table 10 for these IPTs instead. Lobe (and the six-element groupings surrounding the N and W IPTs) powers are relatively unchanged between HEU and LEU cores, as can be seen in the left column of Tables 10 and 11.

This shows that, in all five IPTs evaluated, the neutron flux (fast, thermal, and total) is reduced with the ELF Mk 1A (LEU) fuel compared to the original HEU fuel. This was consistent whether scaled to a 60 MW lobe or not.

Table 10. Neutron flux in IPT pressure tubes for ELF Mk 1A (LEU) fuel.*

Flux Trap (Lobe Power*)	Neutron Flux ($n \cdot cm^{-2} \cdot s^{-1}$) At calculated lobe power			Neutron Flux ($n \cdot cm^{-2} \cdot s^{-1}$) Scaled to 60 (or 45) MW Lobe Power		
	< 1 MeV	> 1 MeV	Total	< 1 MeV	> 1 MeV	Total
N (15.7 MW)	5.98E+14	9.68E+13	6.95E+14	1.72E+15	2.78E+14	1.99E+15
W (17.9 MW)	6.85E+14	1.10E+14	7.95E+14	1.72E+15	2.76E+14	2.00E+15
SW (28.4 MW)	8.41E+14	1.51E+14	9.92E+14	1.78E+15	3.20E+14	2.10E+15
SE (29.5 MW)	8.75E+14	1.58E+14	1.03E+15	1.78E+15	3.20E+14	2.10E+15
NW (17.3 MW)	5.27E+14	1.09E+14	6.36E+14	1.83E+15	3.78E+14	2.20E+15

Table 11. Neutron flux in IPTsfor HEU fuel.

Flux Trap (Lobe Power*)	Neutron Flux ($n \cdot cm^{-2} \cdot s^{-1}$) At calculated lobe power			Neutron Flux ($n \cdot cm^{-2} \cdot s^{-1}$) Scaled to 60 (or 45) MW Lobe Power		
	< 1 MeV	> 1 MeV	Total	< 1 MeV	> 1 MeV	Total
N (15.4 MW)	6.34E+14	1.01E+14	7.35E+14	1.85E+15	2.96E+14	2.15E+15
W (17.9 MW)	7.41E+14	1.17E+14	8.57E+14	1.86E+15	2.93E+14	2.15E+15
SW (28.8 MW)	9.12E+14	1.62E+14	1.07E+15	1.90E+15	3.38E+14	2.24E+15
SE (30.0 MW)	9.52E+14	1.71E+14	1.12E+15	1.90E+15	3.41E+14	2.25E+15
NW (17.6 MW)	5.71E+14	1.16E+14	6.88E+14	1.95E+15	3.97E+14	2.35E+15

Table 12. Percent change in scaled neutron flux in IPTs between HEU and LEU.

Location	Difference in Neutron Fluxes (%) Scaled to 60 (or 45) MW Lobe Power		
	< 1 MeV	> 1 MeV	Total
N	-7.3 ± 0.2	-6.3 ± 0.4	-7.2 ± 0.2
W	-7.5 ± 0.2	-5.6 ± 0.4	-7.2 ± 0.2
SW	-6.4 ± 0.2	-5.4 ± 0.3	-6.3 ± 0.2
SE	-6.6 ± 0.2	-6.2 ± 0.3	-6.5 ± 0.2
NW	-6.3 ± 0.2	-4.8 ± 0.3	-6.0 ± 0.2

* Flux values for SW, SE, and NW flux traps were scaled to 60 MW. In the cases of N and W flux traps, these do not have a true eight-element lobe surrounding them. In these cases, the six adjacent element powers were summed and then scaled to 45 MW for comparison between HEU and LEU.

4.9. IPT Loop Void Worth Comparison

The void reactivity of the IPTs was evaluated using the representative loading of HEU and ELF Mk 1A (LEU) fuels. The N, W, SE and SW IPTs were evaluated by replacing the water in these IPTs with void and comparing the k_{eff} values. Table 13 shows the void worth in pcm and in dollars for the four IPTs evaluated. These results indicate that the loop void has either stayed the same within statistical uncertainty or decreased (become less positive) with the change from HEU to ELF Mk 1A (LEU) fuel.

Table 13. Loop void worth comparison between HEU and ELF Mk 1A (LEU) fuel in representative loading.

Loop Voided	**HEU** (β_{eff} = 0.00701)			**LEU** (β_{eff} = 0.00692)			**Δ (LEU – HEU)** in pcm (± 15 pcm)
	k_{eff} (± 8E-5)	Void Worth (pcm)	Void Worth ($)	k_{eff} (± 6E-5)	Void Worth (pcm)	Void Worth ($)	
None	1.00116	NA	NA	1.02175	NA	NA	NA
N	1.00367	250	0.36	1.02426	240	0.35	-10
W	1.00468	350	0.50	1.02495	306	0.44	-44
SW	1.00662	542	0.77	1.02695	496	0.72	-46
SE	1.00670	550	0.78	1.02733	532	0.77	-18

5. Conclusions

Calculations were performed to further characterize the ELF Mk 1A (LEU) fuel and compare its performance to the current HEU fuel. The conclusions drawn from this work include:

- The reactivity to be held down at BOC for ELF Mk 1A fuel is estimated to be approximately $2.75 greater than with HEU for a typical cycle. This is a combined effect of the absence of burnable poison in the ELF fuel and the reduced neck shim worth in LEU fuel compared to HEU.
- Burnable poison rods were conceptualized for use in the small B positions containing Gd_2O_3 absorber. These were shown to provide $2.37 of negative reactivity at BOC and to burn out in less than half of a cycle.
- Neck shims were found to be worth, on average, slightly less in the LEU core than in the HEU core. The worth of all neck shims simultaneously was calculated to be $0.75 less in the LEU core than in the HEU core.

- The worth of OSCCs is approximately the same between HEU and ELF Mk 1A (LEU) fuels in the representative loading evaluated. This was evaluated by rotating all banks simultaneously.
- The safety rod worth is relatively unchanged between HEU and ELF Mk 1A (LEU) fuels in the representative loading evaluated. However, this should be reevaluated with different loadings.
- Neutron flux in beryllium reflector locations of interest is generally reduced upon changing from HEU to ELF Mk 1A (LEU) fuels in the representative loading evaluated.
- Neutron flux in flux trap locations is generally reduced upon changing from HEU to ELF Mk 1A (LEU) fuels in the representative loading evaluated.
- The IPT loop void reactivity is approximately the same or less positive with ELF Mk 1A (LEU) fuel than HEU in the representative loading evaluated.

Inputs and outputs used in these calculations have been archived via INL's Subversion database:

```
$ svn info
https://hpcsc/svn/ATRPhysics/RERTR/Serpent_Models/ELF_Mk1A/Additional

Path: Additional
URL: https://hpcsc/svn/ATRPhysics/RERTR/Serpent_Models/ELF_Mk1A/Additional
Repository Root: https://hpcsc/svn/ATRPhysics
Repository UUID: 153f5382-2d4e-11e0-9027-c7ef2cc1c428
Revision: 359
Node Kind: directory
Last Changed Author: popema
Last Changed Rev: 359
Last Changed Date: 2014-07-14 10:43:19 -0600 (Mon, 14 Jul 2014)
```

6. References

1. M.A. Pope, "Physics Analysis of the Enhanced LEU Fuel (ELF) Mk 1A Design," ECAR-2471, Idaho National Laboratory, DRAFT.

2. M.A. Pope, "Physics Analysis of the Enhanced LEU Fuel (ELF) Mk 1B Design," ECAR-2472, Idaho National Laboratory, DRAFT.

3. M.A. Pope, "Results of Physics Calculations in Support of RELAP5 Analysis of the Enhanced LEU Fuel (ELF) Mk 1A," ECAR-2469, Idaho National Laboratory, DRAFT.

4. M.A. Pope, "Results of Physics Calculations in Support of RELAP5 Analysis of the Enhanced LEU Fuel (ELF) Mk 1B," ECAR-2470, Idaho National Laboratory, DRAFT.

5. VTT Technical Research Centre of Finland, "Serpent 1.1.7: Continuous Energy Monte Carlo Reactor Physics Burnup Calculation Code," http://www-rsicc.ornl.gov/codes/ccc/ccc7/ccc-757.html.

6. S.S. Kim, B.G. Schnitzler, "Advanced Test Reactor: Serpentine Arrangement of Highly Enriched Water-Moderated Uranium-Aluminide Fuel Plates Reflected by Beryllium", NEA/NSC/DOC/(95)03/II, Volume II, HEU-MET-THERM-022.

7. M. D. DeHart, "Analysis of Candidate LEU Fuel Designs for ATR," ECAR-1997, Idaho National Laboratory, Aug. 29, 2012.

8. SAR-153-4, 2006, "Chapter 4 – Reactor – Upgraded Final Safety Analysis Report for the Advanced Test Reactor," Rev. 10, 4/25/2006. [EDMS Assigned ID: SAR-153-4]

Appendix A - List of Serpent Files used in Calculations

4.1. Alternative Core Loadings

File	*Description*
elf_m1_repdepl2	Alternative loading 2, no external poisons
elf_m1_repdepl3	Alternative loading 3, no external poisons

4.2. Burnable Poison Rods in Small B Positions

File	*Description*
elf_m1_Gad0	Representative loading, no external poisons
elf_m1_Gad1	Representative loading, poisons in B-1 position
elf_m1_Gad2	Representative loading, poisons in B-2 position
elf_m1_Gad3	Representative loading, poisons in B-3 position
elf_m1_Gad4	Representative loading, poisons in B-4 position
elf_m1_Gad5	Representative loading, poisons in B-5 position
elf_m1_Gad6	Representative loading, poisons in B-6 position
elf_m1_Gad7	Representative loading, poisons in B-7 position
elf_m1_Gad8	Representative loading, poisons in B-8 position
elf_m1_Gadall	Representative loading, poisons in B-1 through B-8

4.3. Depletion with External Burnable Poison Pins

File	*Description*
elf_m1_rep2G27	Alternative loading 2, poisons in locations B2-7
elf_m1_rep3G27	Alternative loading 3, poisons in locations B2-7

4.4. Neck Shim Worth Comparison

File	*Description*
elf_m1_shm0	LEU Representative loading, all neck shims withdrawn
elf_m1_shmSW1	LEU Representative loading, neck shim 1 in SW lobe withdrawn
elf_m1_shmSW2	LEU Representative loading, neck shim 2 in SW lobe withdrawn
elf_m1_shmSW3	LEU Representative loading, neck shim 3 in SW lobe withdrawn
elf_m1_shmSW4	LEU Representative loading, neck shim 4 in SW lobe withdrawn
elf_m1_shmSW5	LEU Representative loading, neck shim 5 in SW lobe withdrawn

elf_m1_shmSW6	LEU Representative loading, neck shim 6 in SW lobe withdrawn
elf_m1_shmSE1	LEU Representative loading, neck shim 1 in SE lobe withdrawn
elf_m1_shmSE2	LEU Representative loading, neck shim 2 in SE lobe withdrawn
elf_m1_shmSE3	LEU Representative loading, neck shim 3 in SE lobe withdrawn
elf_m1_shmSE4	LEU Representative loading, neck shim 4 in SE lobe withdrawn
elf_m1_shmSE5	LEU Representative loading, neck shim 5 in SE lobe withdrawn
elf_m1_shmSE6	LEU Representative loading, neck shim 6 in SE lobe withdrawn
elf_m1_shmNE1	LEU Representative loading, neck shim 1 in NE lobe withdrawn
elf_m1_shmNE2	LEU Representative loading, neck shim 2 in NE lobe withdrawn
elf_m1_shmNE3	LEU Representative loading, neck shim 3 in NE lobe withdrawn
elf_m1_shmNE4	LEU Representative loading, neck shim 4 in NE lobe withdrawn
elf_m1_shmNE5	LEU Representative loading, neck shim 5 in NE lobe withdrawn
elf_m1_shmNE6	LEU Representative loading, neck shim 6 in NE lobe withdrawn
elf_m1_shmNW1	LEU Representative loading, neck shim 1 in NW lobe withdrawn
elf_m1_shmNW2	LEU Representative loading, neck shim 2 in NW lobe withdrawn
elf_m1_shmNW3	LEU Representative loading, neck shim 3 in NW lobe withdrawn
elf_m1_shmNW4	LEU Representative loading, neck shim 4 in NW lobe withdrawn
elf_m1_shmNW5	LEU Representative loading, neck shim 5 in NW lobe withdrawn
elf_m1_shmNW6	LEU Representative loading, neck shim 6 in NW lobe withdrawn
elf_m1_shmAll	LEU Representative loading, all neck shims inserted
HEU_shm0	HEU Representative loading, all neck shims withdrawn
HEU_shmSW1	HEU Representative loading, neck shim 1 in SW lobe withdrawn
HEU_shmSW2	HEU Representative loading, neck shim 2 in SW lobe withdrawn
HEU_shmSW3	HEU Representative loading, neck shim 3 in SW lobe withdrawn
HEU_shmSW4	HEU Representative loading, neck shim 4 in SW lobe withdrawn
HEU_shmSW5	HEU Representative loading, neck shim 5 in SW lobe withdrawn
HEU_shmSW6	HEU Representative loading, neck shim 6 in SW lobe withdrawn
HEU_shmSE1	HEU Representative loading, neck shim 1 in SE lobe withdrawn
HEU_shmSE2	HEU Representative loading, neck shim 2 in SE lobe withdrawn
HEU_shmSE3	HEU Representative loading, neck shim 3 in SE lobe withdrawn
HEU_shmSE4	HEU Representative loading, neck shim 4 in SE lobe withdrawn
HEU_shmSE5	HEU Representative loading, neck shim 5 in SE lobe withdrawn
HEU_shmSE6	HEU Representative loading, neck shim 6 in SE lobe withdrawn
HEU_shmNE1	HEU Representative loading, neck shim 1 in NE lobe withdrawn
HEU_shmNE2	HEU Representative loading, neck shim 2 in NE lobe withdrawn
HEU_shmNE3	HEU Representative loading, neck shim 3 in NE lobe withdrawn
HEU_shmNE4	HEU Representative loading, neck shim 4 in NE lobe withdrawn
HEU_shmNE5	HEU Representative loading, neck shim 5 in NE lobe withdrawn
HEU_shmNE6	HEU Representative loading, neck shim 6 in NE lobe withdrawn
HEU_shmNW1	HEU Representative loading, neck shim 1 in NW lobe withdrawn

HEU_shmNW2	HEU Representative loading, neck shim 2 in NW lobe withdrawn
HEU_shmNW3	HEU Representative loading, neck shim 3 in NW lobe withdrawn
HEU_shmNW4	HEU Representative loading, neck shim 4 in NW lobe withdrawn
HEU_shmNW5	HEU Representative loading, neck shim 5 in NW lobe withdrawn
HEU_shmNW6	HEU Representative loading, neck shim 6 in NW lobe withdrawn
HEU_shmAll	HEU Representative loading, all neck shims inserted

4.5. OSCC Worth Comparison

File	***Description***
elf_m1_OS_000	LEU Representative loading, all OSCCs at 0º rotation
elf_m1_OS_010	LEU Representative loading, all OSCCs at 10º rotation
elf_m1_OS_020	LEU Representative loading, all OSCCs at 20º rotation
elf_m1_OS_030	LEU Representative loading, all OSCCs at 30º rotation
elf_m1_OS_040	LEU Representative loading, all OSCCs at 40º rotation
elf_m1_OS_050	LEU Representative loading, all OSCCs at 50º rotation
elf_m1_OS_060	LEU Representative loading, all OSCCs at 60º rotation
elf_m1_OS_070	LEU Representative loading, all OSCCs at 70º rotation
elf_m1_OS_080	LEU Representative loading, all OSCCs at 80º rotation
elf_m1_OS_090	LEU Representative loading, all OSCCs at 90º rotation
elf_m1_OS_100	LEU Representative loading, all OSCCs at 100º rotation
elf_m1_OS_110	LEU Representative loading, all OSCCs at 110º rotation
elf_m1_OS_120	LEU Representative loading, all OSCCs at 120º rotation
elf_m1_OS_130	LEU Representative loading, all OSCCs at 130º rotation
elf_m1_OS_140	LEU Representative loading, all OSCCs at 140º rotation
elf_m1_OS_150	LEU Representative loading, all OSCCs at 150º rotation
elf_m1_OS_160	LEU Representative loading, all OSCCs at 160º rotation
elf_m1_OS_170	LEU Representative loading, all OSCCs at 170º rotation
elf_m1_OS_180	LEU Representative loading, all OSCCs at 180º rotation
HEU_OS_000	HEU Representative loading, all OSCCs at 0º rotation
HEU_OS_010	HEU Representative loading, all OSCCs at 10º rotation
HEU_OS_020	HEU Representative loading, all OSCCs at 20º rotation
HEU_OS_030	HEU Representative loading, all OSCCs at 30º rotation
HEU_OS_040	HEU Representative loading, all OSCCs at 40º rotation
HEU_OS_050	HEU Representative loading, all OSCCs at 50º rotation
HEU_OS_060	HEU Representative loading, all OSCCs at 60º rotation
HEU_OS_070	HEU Representative loading, all OSCCs at 70º rotation
HEU_OS_080	HEU Representative loading, all OSCCs at 80º rotation

HEU_OS_090	HEU Representative loading, all OSCCs at 90º rotation
HEU_OS_100	HEU Representative loading, all OSCCs at 100º rotation
HEU_OS_110	HEU Representative loading, all OSCCs at 110º rotation
HEU_OS_120	HEU Representative loading, all OSCCs at 120º rotation
HEU_OS_130	HEU Representative loading, all OSCCs at 130º rotation
HEU_OS_140	HEU Representative loading, all OSCCs at 140º rotation
HEU_OS_150	HEU Representative loading, all OSCCs at 150º rotation
HEU_OS_160	HEU Representative loading, all OSCCs at 160º rotation
HEU_OS_170	HEU Representative loading, all OSCCs at 170º rotation
HEU_OS_180	HEU Representative loading, all OSCCs at 180º rotation

4.6. Safety Rod Worth Comparison

Files	***Description***
elf_m1_nom	LEU Representative loading, safety rods withdrawn
elf_m1_Nins	LEU Representative loading, N safety rod inserted
elf_m1_Sins	LEU Representative loading, S safety rod inserted
elf_m1_Eins	LEU Representative loading, E safety rod inserted
elf_m1_Wins	LEU Representative loading, W safety rod inserted
elf_m1_SWins	LEU Representative loading, SW safety rod inserted
elf_m1_SEins	LEU Representative loading, SE safety rod inserted
elf_m1_Allins	LEU Representative loading, all safety rods inserted
HEU_nom	HEU Representative loading, safety rods withdrawn
HEU_Nins	HEU Representative loading, N safety rod inserted
HEU_Sins	HEU Representative loading, S safety rod inserted
HEU_Eins	HEU Representative loading, E safety rod inserted
HEU_Wins	HEU Representative loading, W safety rod inserted
HEU_SWins	HEU Representative loading, SW safety rod inserted
HEU_SEins	HEU Representative loading, SE safety rod inserted
HEU_Allins	HEU Representative loading, all safety rods inserted

4.7. Neutron Flux in Beryllium Reflector

File	***Description***
elf_m1_Beflu	LEU Representative loading, beryllium reflector flux tallies
HEU_Beflu	HEU Representative loading, beryllium reflector flux tallies

4.8. Neutron Flux in IPT Pressure Tubes

File	***Description***
elf_m1_IPTflu	LEU Representative loading, IPT flux tallies
HEU_IPTflu	HEU Representative loading, IPT flux tallies

4.9. IPT Loop Void Worth Comparison

File	***Description***
elf_m1_nom	LEU Representative loading, safety rods withdrawn
elf_m1_voidSW	LEU Representative loading, SW IPT voided
elf_m1_voidN	LEU Representative loading, N IPT voided
elf_m1_voidW	LEU Representative loading, W IPT voided
elf_m1_voidSE	LEU Representative loading, SE IPT voided
HEU_nom	HEU Representative loading, safety rods withdrawn
HEU_voidSW	HEU Representative loading, SW IPT voided
HEU_voidN	HEU Representative loading, N IPT voided
HEU_voidW	HEU Representative loading, W IPT voided
HEU_voidSE	HEU Representative loading, SE IPT voided